11th International Conference on Vibration Problems
Z. Dimitrovová *et.al.* (eds.)
Lisbon, Portugal, 9–12 September 2013

NONLINEAR ANALYSIS OF DISK BRAKE SQUEAL BY NORMAL FORM THEORY

Lukas Lentz*[1], Daniel Hochlenert[1]

[1]Chair of Mechatronics and Machine Dynamics Department of Applied Mechanics TU Berlin, Germany
lukas.lentz@tu-berlin.de, daniel.hochlenert@tu-berlin.de

Keywords: nonlinear analysis, brake squeal, normal form.

Abstract. *Brake squeal is generated by friction induced self-excited vibrations of the brake system. The noise free configuration of the brake system loses stability through a flutter type instability and the system starts oscillating in a limit cycle. Usually, the stability analysis of disk brake models, both analytical as well as finite element based, investigates linearized models, i.e. the eigenvalues of the linearized equations of motion. Eigenvalues with positive real parts are interpreted as the onset of squeal. Nonlinearities are commonly neglected due to the high effort associated with the corresponding calculations. However, there are experimentally observed effects not covered by these analyses, even though the full nonlinear models include these effects in principle. The most important, not covered effect is the (quasi-) stationary squealing state itself (a limit cycle oscillation).*

The presen paper describes a nonlinear stability and bifurcation analysis of a disk brake model. The nonlinearities originate from visco-elastic properties of the friction material, which are identified in a special test rig. Using the theory of normal forms, it is shown how nonlinear mathematical-mechanical models having a moderate number of degrees freedom can be analyzed semi-analytically and finally reduced to a low order dynamical system. This nonlinear analysis predicts stability boundaries that are more consistent with experimental results.

1 INTRODUCTION

The main reason for brake squeal are friction-induced self-excited vibrations of the brake system. Whereas the state of the non-squealing brake corresponds to a stable trivial solution of the dynamical system, the squealing state correspond to a non-stable trivial solution of the dynamical system [9].
Road tests and investigations at brake test rigs show various effects that cannot be covered by an ordinary linear stability analysis. One of those effects is that a certain threshold speed of the brake disk is needed to initiate squeal, whereas it is possible to lower the speed of the brake disk of a squealing brake system beyond the threshold speed without affecting the frequency of the noise significantly. Moreover, it is possible to initiate squeal by hitting a non-squealing brake which operates on a brake disk speed below the threshold speed with some tool, a mallet for example. The brake system then stays in a squealing state but ca be brought back to a non squealing state, by temporarily changing the brake pressure [1].
From a mathematical point of view, those observations indicate the coexistence of two stable solutions, namely a trivial solution (the non-squealing state) which looses stability when the speed of the disk is increased above the threshold speed, and a non-trivial stable solution (the squealing state). Since the non-trivial solution shows a periodic behaviour it can be specified as limit cycle.
The investigation of the resulting mathematical model reveals the existence of a pair of complex conjugate eigenvalues with positive real part for distinct parameter configurations. Taking the previous mentioned effects of the brake system into account this indicates the existence of a subcritical Hopf bifurcation of the trivial solution, at which the speed of the brake disk is the bifurcation parameter [8].
While the threshold speed can be determined using the linearized equations of motion the analysis of the bifurcation behaviour requires an investigation of the nonlinear equations of motion.
The present paper is based on a nonlinear disk brake model including the brake disk, the brake pads, the caliper and the yoke with 14 degrees of freedom in total. After a short overview of the modeling process a linear analysis is performed to obtain the threshold speed, followed by a nonlinear analysis to reproduce the bifurcation behaviour. In contrast to the previous work on the same topic [3] the nonlinear analysis is carried out using normal form theory without previous center manifold reduction. Therefore it is explained how normal form theory yields a dimensional reduction of the dynamical system which is comparable to the reduction that can be obtained using central manifold theory.

2 MATHEMATICAL-MECHANICAL MODELING

The model used for the investigations described in the present paper is virtually indentical to the model described in [3] and is for this reason only discussed briefly. The disk brake model shown in figure 1 includes the brake disk (1), the pads (2), the caliper (3) and the yoke (4). Based on [5] the the brake disk is modeled as a rotating annular Kirchhoff plate assuming a constant speed of rotation Ω.
Since a real brake disk is not a homogenous plate in the sense of Kirchhoff's theory, the plate's parameters are experimentally identified to match the dynamical behavior of the real break disk in the frequency range of interest [6]. The discretization of the disk is performed using a pair of eigenfunctions of the corresponding nonrotating Kirchhoff plate [3].
The back plates of the pads are modeled as rigid bodies and restricted to movements in the circumferential and normal directions of the undeformed plate only.

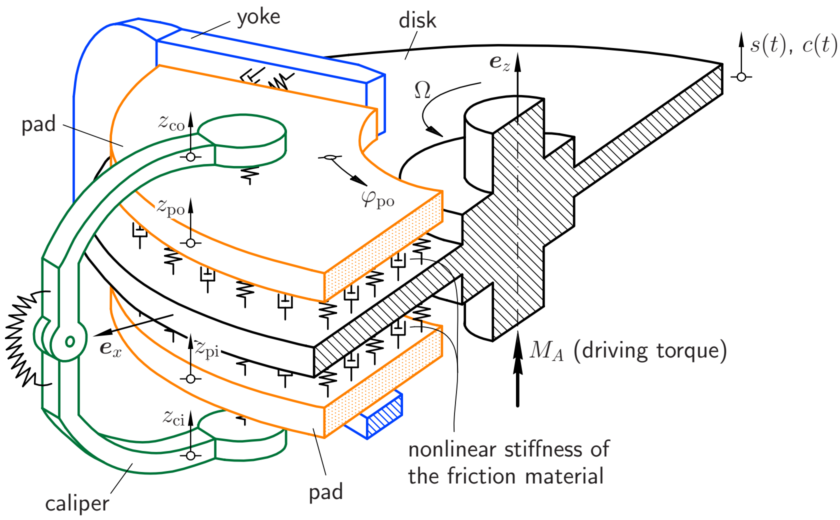

Figure 1: Mechanical Model of disk brake [3]

The brake lining is represented by a massless pointwise nonlinear viscoelastic material, such that the formulation of the frictional contact described in [5] can be adapted by integration over the area of the brake pads. The caliper as well as the yoke are modeled as systems of point masses connected by rigid massless bars, joints, elastic springs and viscous damping elements. Since the vibrational displacements occurring during squeal are in the range of micrometers, the modell is geometrically linearized so that the stiffness characteristic of the brake lining irepresents the only origin of nonlinearity.

The derivation of the equations of motion is out of scope of the present paper and can be found in [2] and [5]. The resulting system of autonomous second-order differential equations can be written as

$$\boldsymbol{M}\ddot{\boldsymbol{u}} + (\boldsymbol{D} + \boldsymbol{G})\dot{\boldsymbol{u}} + (\boldsymbol{K} + \boldsymbol{N})\boldsymbol{u} + \boldsymbol{f}_{nl}(\boldsymbol{u}, \dot{\boldsymbol{u}}) = \boldsymbol{0}, \tag{1}$$

where $\boldsymbol{M}, \boldsymbol{D}, \boldsymbol{G}, \boldsymbol{K}, \boldsymbol{N} \in \mathbb{R}^{14\times14}$ and $\boldsymbol{u} \in \mathbb{R}^{14}$. $\boldsymbol{f}_{nl} : \mathbb{R}^{28} \mapsto \mathbb{R}^{14}$ gathers all nonlinearities resulting from the nonlinear characteristic of the brake lining.

The gyroscopic matrix $\boldsymbol{G}$ is typical for the description of a rotating continuum in an inertial coordinate system. The circulatory matrix $\boldsymbol{N}$ originates from nonconservative forces in the contact area between the brake disk and the pads. The interaction of gyroscopic and nonconservative forces makes the system highly susceptible to self-excited vibrations.

Prior to the further investigation, the system (1) is transformed to a system of first-order differential equations, in which the rotational speed of the brake disk Ω is included as a trivial state variable [4]. Introducing $\boldsymbol{q} = [\boldsymbol{u}, \dot{\boldsymbol{u}}, \Omega]^T \in \mathbb{R}^{29}$, (1) yields

$$\dot{\boldsymbol{q}} = \boldsymbol{f}(\boldsymbol{q}) \ . \tag{2}$$

.

3 NORMAL FORM TRANSFORMATION

Consider the system of autonomous ordinary differential equations in the form of (2)

$$\dot{\boldsymbol{q}} = \boldsymbol{f}\left(\boldsymbol{q}\right),\ \boldsymbol{q} \in \mathbb{R}^n,\ \boldsymbol{f} : \mathbb{R}^n, \to \mathbb{R}^n\ . \tag{3}$$

Supposing that $\boldsymbol{f}$ has a point of equilibrium in $\boldsymbol{0}$ and is sufficiently differentiable, (3) can be localy approximated by its taylor polynomial

$$\dot{\boldsymbol{q}} = \boldsymbol{A}\boldsymbol{q} + \boldsymbol{f}^2(\boldsymbol{q}) + \boldsymbol{f}^3(\boldsymbol{q}) + \dots \tag{4}$$

in which all monomials of grade i are combined in $\boldsymbol{f}^i$.
In case all eigenvalues $\lambda_i,\ i = 1, \dots, n$ of $\boldsymbol{A}$ are simple or semisimple the existence of an invertible matrix $\boldsymbol{R}$ with the property

$$\boldsymbol{R}^{-1}\boldsymbol{A}\boldsymbol{R} =: \boldsymbol{\Lambda} = diag\left[\lambda_1, \dots, \lambda_n\right] \tag{5}$$

is guaranteed. Applying the corresponding linear tranformation

$$\boldsymbol{q} = \boldsymbol{R}\boldsymbol{x} \tag{6}$$

on system (4) yields a decoupling in the linear terms

$$\dot{\boldsymbol{x}} = \boldsymbol{\Lambda}\boldsymbol{x} + \hat{\boldsymbol{f}}^2(\boldsymbol{x}) + \hat{\boldsymbol{f}}^3(\boldsymbol{x}) + \dots =: \hat{\boldsymbol{f}}(\boldsymbol{x})\ , \tag{7}$$

in which the abbreviation $\hat{\boldsymbol{f}}^i(\boldsymbol{x}) = \boldsymbol{R}^{-1}\boldsymbol{f}^i(\boldsymbol{R}\boldsymbol{x})$ is used. The goal is now to further simplify (7) using the nonlinear near-identity transformation

$$\boldsymbol{x} = \boldsymbol{y} + \boldsymbol{g}^2(\boldsymbol{y}) + \boldsymbol{g}^3(\boldsymbol{y}) + \dots =: \boldsymbol{g}(\boldsymbol{y})\ . \tag{8}$$

As it will be shown later, it is possible to construct the transformation (8) in such a way that the transformed system

$$\dot{\boldsymbol{y}} = \boldsymbol{\Lambda}\boldsymbol{y} + \boldsymbol{h}^2(\boldsymbol{y}) + \boldsymbol{h}^3(\boldsymbol{y}) + \dots =: \boldsymbol{h}(\boldsymbol{y})\ , \tag{9}$$

which from now on will be referred to as normal form, is to some extend decoupled in the non-linear terms. For the further description of the properties of $\boldsymbol{h}$ and $\boldsymbol{g}$ it is convenient to consider each term component-wise.
Let $\boldsymbol{\alpha} := (\alpha_1, \alpha_2, \dots, \alpha_n) \in \mathbb{N}^n$ be a multi index, $|\boldsymbol{\alpha}| := \alpha_1 + \dots + \alpha_n$ its length and $\boldsymbol{A}_p := \{\boldsymbol{\alpha} \in \mathbb{N}^n : |\alpha| = p\}$ the set of all multi indices with length p. Then, for instance the i-th component of the term $\boldsymbol{h}^m$, in which all m-th order monomials of $\boldsymbol{h}$ are gathered, can be written as

$$h_i^m = \sum_{\boldsymbol{\alpha} \in \boldsymbol{A}_m} h_{i,\boldsymbol{\alpha}}^m \prod_{j=1}^{n} y_j^{\alpha_j}\ , \tag{10}$$

where h_i^m is uniquely determined by its coefficients $h_{i,\boldsymbol{\alpha}}^m \in \mathbb{R}$. In [7] it is shown that the coefficients are given by the equation

$$h_{i,\boldsymbol{\alpha}}^m = \tilde{f}_{i,\boldsymbol{\alpha}}^m + g_{i,\boldsymbol{\alpha}}^m \left(\lambda_i - \sum_{j=1}^{n} \alpha_j \lambda_j\right)\ . \tag{11}$$

Since the calculation of $\tilde{f}^m_{i,\boldsymbol{\alpha}}$ requires only m-th order terms of $\hat{\boldsymbol{f}}$ and $(m-1)$-th order terms of $\boldsymbol{g}$ and $\boldsymbol{h}$ equation (12) can be used to calculate the tranformation $\boldsymbol{g}$ and the corresponding normal form $\boldsymbol{h}$ in an iterative manner. The determining part is the term in parentheses on the right hand side of equation (12) which is referred to as resonance condition [8]. Two different cases can be distinguished

$$\begin{aligned} &i) \text{ If } \ \lambda_i = \sum_{j=1}^{n} \alpha_j \lambda_j, \ \text{ set } \ h^m_{i,\boldsymbol{\alpha}} = \tilde{f}^m_{i,\boldsymbol{\alpha}} \ \text{ and } \ g^m_{i,\boldsymbol{\alpha}} = 0 \, . \\ &ii) \text{ If } \ \lambda_i \neq \sum_{j=1}^{n} \alpha_j \lambda_j, \ \text{ set } \ h^m_{i,\boldsymbol{\alpha}} = 0 \ \text{ and } \ g^m_{i,\boldsymbol{\alpha}} = \frac{\tilde{f}^m_{i,\boldsymbol{\alpha}}}{\sum\limits_{j=1}^{n} \alpha_j \lambda_j - \lambda_i} \, . \end{aligned} \tag{12}$$

As already mentioned in the introduction, the investigated system possesses a pair of complex conjugate eigenvalues (λ_r, λ_s), $1 \leq r < s \leq n$ which obtain a possitive real part for certain parameter configurations. Since the real part of all other eigenvalues is strictly negative, the resonance condition can only be fulfilled for $\lambda_i = \lambda_r$ (this applies analogously to the case $\lambda_i = \lambda_s$) if

$$\lambda_r = \frac{m+1}{2}\lambda_r + \frac{m-1}{2}\lambda_s \tag{13}$$

holds. This directly implies that

$$g^m_r = 0, \quad \text{and} \quad h^m_r = \begin{cases} 0, & m \text{ even} \\ \tilde{f}^m_{r,\boldsymbol{\alpha}} y_r^{(\frac{m+1}{2})} y_s^{(\frac{m-1}{2})}, & m \text{ uneven} \end{cases} . \tag{14}$$

Hence, as noted above, the transformation $\boldsymbol{g}$ completely decouples the coordinates y_r and y_s, corresponding to the critical eigenvalues (λ_r, λ_s), from the coordinates corresponding to non-critical eigenvalues. For the investigation of the bifurcation behavior it is sufficient to investigate the two-dimensional system

$$\dot{\begin{pmatrix} y_r \\ y_s \end{pmatrix}} = \begin{pmatrix} \lambda_r y_r \\ \lambda_s y_s \end{pmatrix} + \begin{pmatrix} k_1^3 y_r^2 y_s \\ k_2^3 y_r y_s^2 \end{pmatrix} + \begin{pmatrix} k_1^5 y_r^3 y_s^2 \\ k_2^5 y_r^3 y_s^2 \end{pmatrix} + \dots \, , \tag{15}$$

which implies a significant reduction of complexity. A further simplification can be achieved using the polar coordinates $y_r = re^{\mathrm{i}\phi}$, $y_s = re^{-\mathrm{i}\phi}$. The resulting differential equations for r and φ are

$$\begin{pmatrix} \dot{r} \\ \dot{\phi} \end{pmatrix} = \begin{pmatrix} 0 \\ \frac{1}{2\mathrm{i}}(\lambda_r - \lambda_s) \end{pmatrix} + \begin{pmatrix} \frac{r^3}{2}(k_1^3 + k_2^3) \\ \frac{r^2}{2\mathrm{i}}(k_1^3 - k_2^3) \end{pmatrix} + \begin{pmatrix} \frac{r^5}{2}(k_1^5 + k_2^5) \\ \frac{r^4}{2\mathrm{i}}(k_1^5 - k_2^5) \end{pmatrix} + \dots \, . \tag{16}$$

The stationary points r_i^* of

$$\dot{r} = r^3 \left(\frac{1}{2}(k_1^3 + k_2^3) + \frac{r^2}{2}(k_1^5 + k_2^5) + \dots \right) \tag{17}$$

correspond to periodic solutions (limit cycles) of the investigated system, since the flux of r does not depend on φ. Substituion of r^* in the polar coordinates yields the corresponding y_r^* and y_s^*. All other coordinates vanish over time, i.e. $y_i = 0, i \neq r, s$. Substitution of $\boldsymbol{y}^*$ in (8) yields the limit cycles in modal coordinates

$$\boldsymbol{x}^* = \boldsymbol{g}([0, \dots, 0, y_r^*, y_s^*, 0, \dots, 0]^T) \tag{18}$$

which can be transformed in physical coordinates using the linear transformation (6).
In respect to practiacal applicabilty it is worth mentioning that the normal form transformation requires comprehensive computations. Hence it is reasonable to include paramters, such as the bifurcation parameter, in the transformation. This approach leads to additional zero eigenvalues which need to be considered in the evaluation of the resonance condition.

4 STABILITY ANALYSIS

The nonlinear dynamical system (2) resulting from the mechanical model of the brake system and the corresponding normal form are to large to be shown in a meaningful way. Instead, the qualitative characteristics will be described using symbolic notation wherever applicable.
The analysis consists of two different tasks. First the threshold speed Ω_{lin}, indicating the onset of instability of the trivial solution is determined by a linearization of the equations of motion. Afterwards normal form theory is used to obtain a dimension reduction resulting in a two-dimensional system which contains all the information needed to investigate the bifurcation behavior. As a result, the threshold speed Ω_c, corresponding to two coexisting stable solutions, is determined.

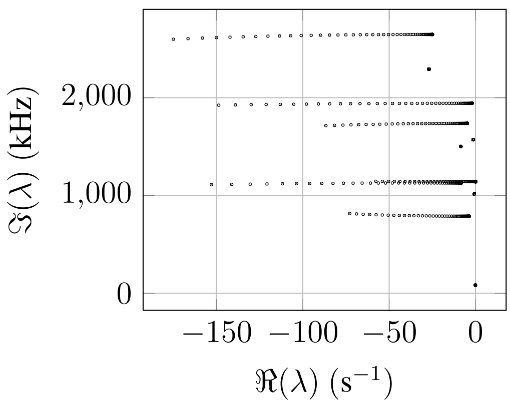

Figure 2: Root locus for varying speed of rotation Ω (only eigenvalues with positive imaginary part)

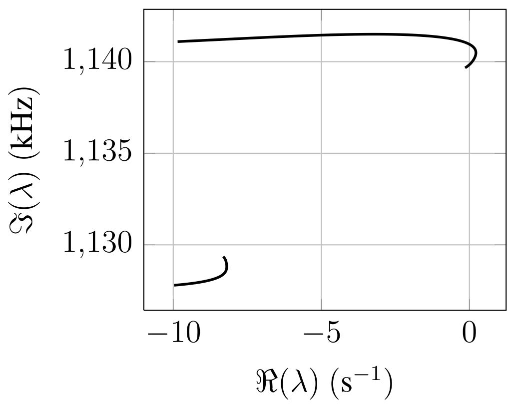

Figure 3: Detailed Root locus for varying speed of rotation Ω (only eigenvalues with positive imaginary part)

For the determination of Ω_{lin} the path of the eigenvalues in the complex plane is investigated for varying speeds of rotation Ω in the range $0.5\pi\ \mathrm{s}^{-1} \leq \Omega \leq 15\pi\ \mathrm{s}^{-1}$. As shown in figure 2, and in detail in figure 3, all eigenvalues have a negative real part except one pair of complex conjugate eigenvalues which has a positive real part for $\Omega > 1.03\pi\ \mathrm{s}^{-1}$. Since the occurence of a positive real part indicates an unstable trivial solution, this yields the threshold speed $\Omega_{\text{lin}} = 1.03\pi\ \mathrm{s}^{-1}$.
Prior to the determination of Ω_c, the normal form of (2) is calculated up to terms of 5-th order using the algorithm presented in [7]. As stated above, the bifurcation behavior of the system in normal form is governed by two coordinates which are decoupled from the remaining coordinates. The introduction of polar coordinates $y_r = re^{\mathrm{i}\phi},\ y_s = re^{-\mathrm{i}\phi}$ yields the differential equations

$$\dot{r} = h_r(r, \Omega), \tag{19a}$$

$$\dot{\varphi} = h_\varphi(r, \Omega). \tag{19b}$$

Since the flux of (19a) is independent of φ, stationary points of (19a) correspond to periodic solutions of (2). In addition to the trivial solution r_0, two non-trivial stationary points r_1 and r_2

(corresponding to limit cycles) exist, which are depicted in figure 4 for varying speed Ω.
The stability of the trivial solution r_0 can be determined using figure 3 since it corresponds to the trivial solution of the dynamic system. As a result r_0 is stable for $\Omega < \Omega_{\text{lin}}$ and unstable for $\Omega > \Omega_{\text{lin}}$.

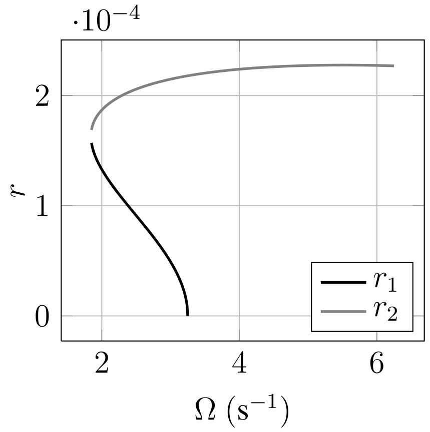

Figure 4: Non-trivial stationary points r_1 and r_2 of (19a) for varying speed Ω

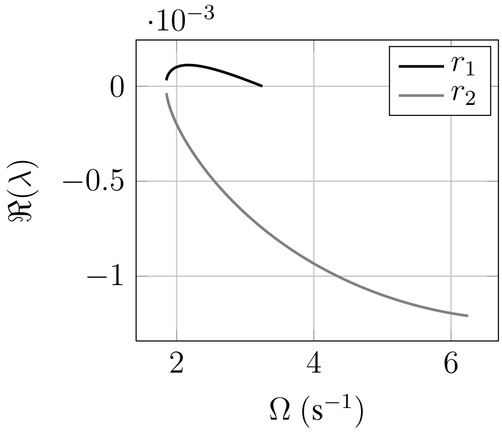

Figure 5: Real part of the eigenvalues of the modified differential equations (20) used to determine the stability of r_1 and r_2 for varying speed Ω

In order to analyse the stability of the non-trivial solutions, the modified differential equations

$$\dot{z}_i = h_r(z_i + r_i) - h_r(r_i),\ i = 1, 2 \tag{20}$$

where $z_i = r - r_i$, can be used since the stability of the trivial solutions of (20) is equivalent to the stability of the non-trivial solutions r_1 and r_2. In figure 5 the real part of the particular eigenvalues of (20) is shown. As can be seen r_1, is an unstable and r_2 a stable solution. Hence, the threshold speed $\Omega > 0,59\pi\ \mathrm{s}^{-1}$ for the existence of two parallel stable solutions can therefore be taken from figure 4. For a further interpretation of the results, a backward transformation of

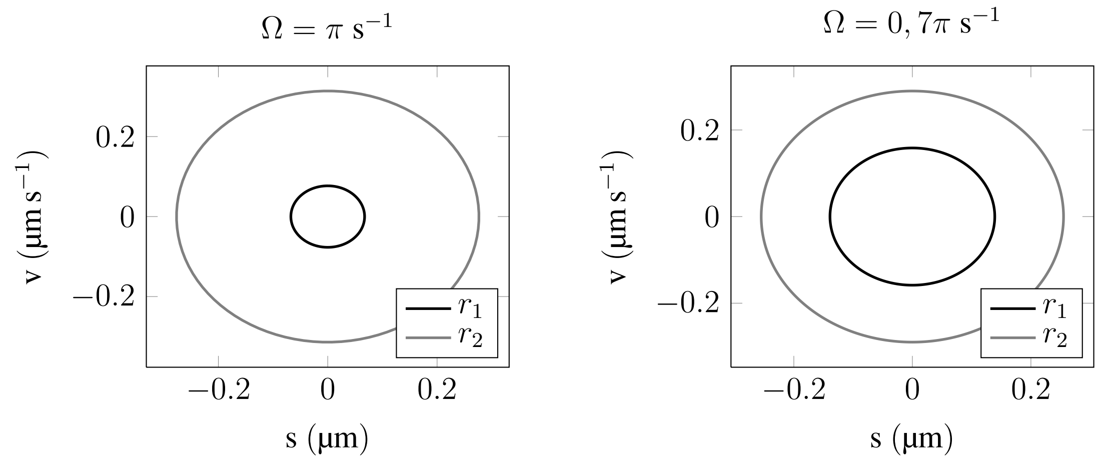

Figure 6: Limit cycles in physical coordinates for $\Omega = \pi\ \mathrm{s}^{-1}$ and $\Omega = 0,7\pi\ \mathrm{s}^{-1}$

the limit cycles corresponding to r_1 and r_2 to physical coordinates is performed. Substituting those coordinates in the discretization of the break disk, the axial displacement and velocity for every point on the break disk can be determined. As a example the phase portraits for rotational speeds $\Omega = \pi\ \mathrm{s}^{-1}$ and $\Omega = 0,7\pi\ \mathrm{s}^{-1}$ are shown in figure 6.

5 CONCLUSIONS

A nonlinear stability analysis of a realistic disk brake model is described in the present paper. The investigation of the existing Hopf bifurcation shows, that for a rotational speed of the brake disk between the threshold speeds Ω_c and Ω_{lin}, a stable non-trivial solution (limit cycle, squealing state of the brake) coexists with the stable trivial solution (non-squealing state of the disk), while for a rotational speed of the brake disk above Ω_{lin} the trivial solution becomes unstable. This result is in good agreement with the operating experience, since it can be used to explain several experimentally observed effects, that are not covered by a linear stability analysis.
From the practical point of view, it is shown that a exclusive use of the normal form transformation yields a system reduction, which can be compared to the system reduction, which is obtained using center manifolds in combination with a normal form transformation [3]. Beside the advantage of less complex computations, the exclusive use of normal form transformation gives rise to a semi-analytical computation of the domains of attraction for the stable solutions, as shown in [4].

References

[1] Oliviero Giannini, Adnan Akay, and Francesco Massi. Experimental analysis of brake squeal noise on a laboratory brake setup. *Journal of Sound and Vibration*, 292:1–20, 2006.

[2] Daniel Hochlenert. *Selbsterregte Schwingungen in Scheibenbremsen: Mathematische Modellbildung und aktive Unterdrückung von Bremsenquietschen*. 2006. Dissertation Technische Universität Darmstadt.

[3] Daniel Hochlenert. Nonlinear Stability Analysis of a Disk Brake Model. *Nonlinear Dynamics*, 58:63–73, 2009. 10.1007/s11071-008-9461-0.

[4] Daniel Hochlenert. *Normalformen und Einzugsbereiche nichtlinearer dynamischer Systeme*. 2012. Habilitationsschrift Technische Universität Berlin Institut für Mechanik.

[5] Daniel Hochlenert, Gottfried Spelsberg-Korspeter, and Peter Hagedorn. Friction induced vibrations in moving continua and their application to brake squeal. *Journal of Applied Mechanics*, 74(3):542–549, 2007.

[6] Thira Jearsiripongkul. *Squeal in Floating Caliper Disk Brakes: A Mathematical Model*. Forschen und Wissen - Mechanik. GCA-Verlag, 2005.

[7] Lukas Lentz. *Implementierung der Poincare-Dulac Normalformtransformation für große parameterabhängige Systeme*. 2013. Masterarbeit Technische Universität Berlin Institut für Mechanik.

[8] Hans Troger and Alois Steindl. *Nonlinear Stability and Bifurcation Theory*. Springer, 1991.

[9] Utz von Wagner and Stefan Schlagner. On the origin of disk brake squeal. 2008. to appear in the International Journal of Vehicle Design.